A piecewise-constant binary model for electrical impedance tomography*

UCLA CAM Report 07-04, February 2007

Nicolay M. Tanushev

Department of Mathematics
University of California, Los Angeles
405 Hilgard Avenue
Los Angeles, CA 90095-1555, USA

Luminita A. Vese

Department of Mathematics
University of California, Los Angeles
405 Hilgard Avenue
Los Angeles, CA 90095-1555, USA

Abstract

In this paper, we consider the electrical impedance tomography problem in a computational approach. This inverse problem is the recovery of the electrical conductivity σ in a domain from boundary measurements, given in the form of the Neumann-to-Dirichlet map. We formulate the inverse problem as a variational one, with a fitting term and a regularization term. We restrict the minimization with respect to the unknown σ to piecewise-constant functions defined on rectangular domains in two dimensions. We borrow image segmentation techniques to solve the minimization problem. Several experimental results of conductivity reconstruction from synthetic data are shown, with and without noise, that validate the proposed method.

1 The mathematical problem

Electrical Impedance Tomography (EIT) is a non-invasive inverse method which attempts to determine the electrical conductivity σ of a medium in a domain Ω, by making voltage and current measurements at the boundary, $\partial\Omega$, of the medium. In mathematical terms, the EIT problem is the recovery of the coefficient σ of an elliptic partial differential equation, defined for $x \in \Omega$, given knowledge of the Cauchy data, i.e. the Neumann-to-Dirichlet map or the Dirichlet-to-Neumann map. The EIT problem has important applications in fields such as medical imaging, non-destructive testing of materials, environmental cleaning, geophysics, etc. In the

*This research was supported in part by an Alfred P. Sloan fellowship, by the National Institute of Health through the NIH Roadmap for Medical Research (Grant U54 RR021813 entitled Center for Computational Biology CCB), and by the National Science Foundation Grants NSF ITR 0113439, NSF DMS 0312222, NSF Vigre DMS-0502315.

last two decades, it has been the topic of many theoretical and numerical studies. However, there are still important questions, such as improving the stability of reconstruction algorithms, improving the resolution and reliability of reconstructions of σ, and increasing the speed of inversion algorithms so σ can be imaged in real time [3].

1.1 The Forward Problem

For a known isotropic electrical conductivity function $\sigma \in L^\infty(\Omega)$ (scalar valued, strictly positive and bounded in Ω), we can define the Neumann-to-Dirichlet map, Λ_σ, for a bounded and simply connected domain Ω in the following way. Let u, called the potential, be the solution to the partial differential equation,

$$\begin{aligned} \nabla \cdot \sigma \nabla u &= 0 && \text{in } \Omega \\ \sigma \frac{\partial u}{\partial \nu} &= I && \text{on } \partial\Omega \\ \int_{\partial\Omega} u \, dS &= 0, \end{aligned} \tag{1}$$

where ν is the unit outward normal to $\partial\Omega$ and $\frac{\partial u}{\partial \nu} = \nabla u \cdot \nu$. The function I is restricted to be such that $\int_{\partial\Omega} I \, dS = 0$. This Neumann boundary value problem, referred to as the forward problem, has a unique solution $u \in H^1(\Omega)$ (at least in the weak sense), given that $I \in H^{-1/2}(\partial\Omega)$ (the potential is unique up to an additive constant, that we fix by imposing the condition $\int_{\partial\Omega} u dS = 0$).

The Neumann-to-Dirichlet operator $\Lambda_\sigma : \{I \in H^{-1/2}(\partial\Omega), \int_{\partial\Omega} I dS = 0\} \to H^{1/2}(\partial\Omega)$, maps the Neumann boundary data I to the restriction (trace) of u to the boundary of Ω:

$$\Lambda_\sigma I = u|_{\partial\Omega}.$$

This map depends nonlinearly on the conductivity σ. The Dirichlet-to-Neumann map can also be considered, $\Lambda_\sigma^{-1} : H^{1/2}(\partial\Omega) \to H^{-1/2}(\partial\Omega)$ with $\Lambda_\sigma^{-1} V = \sigma \frac{\partial u}{\partial \nu}$, where $u = V$ on $\partial\Omega$.

1.2 The Inverse Problem

The inverse conductivity problem, as formulated by Calderón [8], is to find a bounded, strictly positive function $\sigma(x)$, given the map Λ_σ^{-1}. Theoretically, this problem can be solved uniquely for a large class of functions σ, as established in [2], [27], [20], [15], [16], [6], and [23] (we highlight in particular the more recent work [2], in two dimensions, where only the above assumptions on Ω and σ are imposed). We will assume knowledge of the Λ_σ rather than Λ_σ^{-1}, since in practice it is less sensitive to noise. Thus, we want to recover a function $\sigma \in L^\infty(\Omega)$, satisfying $\sigma(x) \geq \sigma_0 > 0$ in Ω, given I and $V = u|_{\partial\Omega}$.

We introduce the adjoint potential, τ, as the unique solution to the following problem (called the adjoint problem),

$$\begin{aligned} \nabla \cdot \sigma \nabla \tau &= 0 && \text{in } \Omega \\ \sigma \frac{\partial \tau}{\partial \nu} &= u|_{\partial\Omega} - V && \text{on } \partial\Omega \\ \int_{\partial\Omega} \tau \, dS &= 0. \end{aligned} \tag{2}$$

Here u is the solution to the forward problem (1) and $V \in H^{1/2}(\partial\Omega)$ is such that $\int_{\partial\Omega} V \, dS = 0$. The adjoint potential will be useful in later sections.

1.3 Piecewise-constant image segmentation model

Here, we briefly review the piecewise-constant segmentation method, called "active contours without edges", introduced in [9], [10]. This method will be used to recover the conductivity σ in the next section. Based on the piecewise-constant minimal partition problem of Mumford and Shah [19], the authors in [9], [10] have proposed implicit curve evolution techniques propagating with non-local terms, to solve particular cases of the minimal partition problem. In this problem [19], an image $f : \Omega \to R$ is partitioned into several regions Ω_i, such that the gray-scale level in each Ω_i is close to an average constant c_i. This can also be seen as an inverse problem, and can be accomplished by minimizing the energy functional [19],

$$E^{MS}(\sigma, C) = \lambda \sum_i \int_{\Omega_i} |f(x) - c_i|^2 dx + \mu \text{ Length}(C), \tag{3}$$

where μ and λ are tuning parameters, C is a piecewise smooth curve that partitions Ω into Ω_i, and $\sigma = c_i$ is constant in each Ω_i. A simple observation shows that for a fixed C, the value of c_i that minimizes this functional is given by the average of f over Ω_i. The function $\sigma(x) = \sum_i c_i \chi_{\Omega_i}(x)$ will be an "optimal" piecewise-constant approximation of f. In practice, however, it is difficult to minimize the functional (3). For particular cases, when σ takes a finite number of values c_i, the minimal partition problem can be put in the variational level set framework from [31], [22], [13], [14], in the following way [9], [10]. Suppose that we are working in the simplified case of binary segmentation. The image f can be partitioned using a Lipschitz-continuous function ϕ into two regions, one region where $\phi > 0$ and another where $\phi < 0$. The zero level-line of ϕ will define the curve $C = \{x \in \Omega : \ \phi(x) = 0\}$. Thus $\Omega = \{\phi(x) > 0\} \cup \{\phi(x) < 0\} \cup \{\phi(x) = 0\}$. The length of C will be given by $\text{Length}(C) = \int_\Omega |\nabla H(\phi)| dx = \int_\Omega \delta(\phi)|\nabla\phi| dx$, where H is the Heaviside function and δ is the Dirac delta function. In this case, the functional (3) can be rewritten as [9], [10],

$$\begin{aligned} E^{CV}(c_1, c_2, \phi) &= \lambda \int_\Omega \Big[|f(x) - c_1|^2 H(\phi(x)) + |f(x) - c_2|^2 (1 - H(\phi(x))) \Big] dx \\ &+ \mu \int_\Omega \delta(\phi) |\nabla\phi| dx. \end{aligned}$$

Following the observation from the previous paragraph, the optimal constants c_1 and c_2 for a fixed ϕ are given by

$$c_1 = \frac{\int_\Omega f(x) H(\phi(x)) dx}{\int_\Omega H(\phi(x)) dx}, \qquad c_2 = \frac{\int_\Omega f(x)(1 - H(\phi(x))) dx}{\int_\Omega (1 - H(\phi(x))) dx}. \tag{4}$$

Introducing an artificial time, $t \geq 0$, one verifies that with $\phi(x, t)$ satisfying

$$\frac{\partial\phi}{\partial t} = \delta(\phi) \Big[\mu \text{div}\Big(\frac{\nabla\phi}{|\nabla\phi|} \Big) - \lambda |f - c_1|^2 + \lambda |f - c_2|^2 \Big] \quad \text{in} \quad \Omega \tag{5}$$

$$\frac{\partial\phi}{\partial\nu} = 0 \quad \text{on} \quad \partial\Omega, \tag{6}$$

E^{CV} will be a non-increasing function of t. Extensions to piecewise-constant segmentation with more than two regions and piecewise-smooth segmentation, in a variational multiphase approach, have been introduced in [30]. Related work for region-based segmentation and partitioning was done by [29], [28], [25], together with other references mentioned in [30].

1.4 Related Prior Work

We mention that L. Rondi and F. Santosa have previously applied the Ambrosio-Tortorelli approximations [1] of the general Mumford-Shah problem [19] to the inverse conductivity problem in an elegant work [24], where σ is recovered from an energy minimization formulation with data fidelity term and regularizing term. The authors give theoretical results of existence of piecewise-smooth minimizers σ in $SBV(\Omega)$, and show convergence of the elliptic approximations by Γ-convergence. Our proposed computational method is thus different from the method proposed in [24], because we use the level set approach to minimize the Mumford and Shah functional for the simpler (although more restrictive) piecewise-constant binary segmentation case.

Segmentation techniques for recovering the conductivity σ and other elliptic equation coefficients have been proposed by T. Chan, E. Chung, and X.C. Tai [11], [12] using approaches similar to the approach in this paper. The work [11] considers a different, but related inverse problem; it applies a slightly modified version of the piecewise-constant segmentation method from [9], [10], [30] to recover the coefficient $q(x)$ from an elliptic PDE, by using the total variation, $\int_\Omega |\nabla q| dx$, as a regularization, instead of the length regularization. The work [12] (that much inspired this work) addresses the problem of inverse conductivity; it uses a binary piecewise-constant segmentation method, as in [9], [10], but the regularization is again the total variation. In this work, we show that the length term of the discontinuity set of σ is sufficient to recover σ with high accuracy and smaller jumps, and is simpler in the piecewise-constant case; also, our computational results need about 200-250 iterations for convergence to steady-state instead of 200 - 50000 iterations in [12]; finally, we also show that interior contours (or holes) of the conductivity σ can also be detected by the proposed approach.

The work of L. Borcea et al. [4] also uses a variational approach with regularization to recover the conductivity σ, but in a different way from the present approach.

Our work was much motivated by all the above-mentioned approaches [24], [11], [12], [4].

Other related work, some very recent, can be found in [26], [18], [17], [21], [7], [4], [3], and [5].

2 Formulation of the Minimization

In practice, we do not completely know the Neumann-to-Dirichlet or Dirichlet-to-Neumann map. Instead, we are given a set of N evaluations of the map. Therefore, we assume that Λ_{σ^*} is known for N functions for the true conductivity σ^*. That is, there are N pairs of functions (I_n, V_n) such that $\Lambda_{\sigma^*} I_n = V_n$. Experimentally, this is accomplished by setting a current excitation pattern I_n and measuring the resulting voltage V_n at discrete locations of the electrodes along the boundary $\partial\Omega$.

In practice, the EIT problem is to find σ^* from partial and usually noisy knowledge of Λ_{σ^*}. A significant difficulty is the severe ill-posedness of EIT. This problem is ill-posed in the sense that small perturbations of the boundary data are exponentially amplified in the image of σ inside Ω [3]. Therefore, in the reconstruction process, we have to restrict σ to a subset of $L^\infty(\Omega)$, of smoother functions, as in [4], [24], [11], [12], among others.

In order to obtain a numerical solution to the inverse conductivity problem, we formulate it as a minimization: the functional to be optimized will consist of a data fidelity term (fitting term), and of a regularization term. Using the ideas of the minimal partition problem and piecewise-constant reconstruction [19], [9], [10] in a level set framework, in the simplified case of piecewise constant σ, taking two values, we let

$$\sigma(\phi, c_1, c_2) = c_1 + (c_2 - c_1)H(\phi),$$

where ϕ is the level set function, c_1 and c_2 are the constant values of the conductivity, and H is the Heaviside function. Therefore, motivated by the classical Mumford and Shah functional [19] and its binary level set forms [9], [10], we minimize the energy functional,

$$E(\phi, c_1, c_2) = F(\sigma(\phi, c_1, c_2)) + \alpha(F)L(\phi),$$

where the fitting term and the regularizing length term are given respectively by,

$$\begin{aligned} F(\sigma) &= \sum_{n=1}^{N} \frac{\|\Lambda_\sigma I_n - V_n\|^2_{L^2(\partial\Omega)}}{N\|V_n\|^2_{L^2(\partial\Omega)}}, \\ L(\phi) &= \int_\Omega |\nabla H(\phi)|dx = \int_\Omega \delta(\phi)|\nabla\phi|dx, \end{aligned}$$

with $\alpha(s)$ a non-decreasing function such that $\alpha(0) = 0$. This function allows us to control the size of the regularization. Note that under these restrictions on α, we automatically have that the true conductivity $\sigma^* = \sigma(\phi^*, c_1^*, c_2^*)$ is an absolute minimum of the functional, as $E(\phi^*, c_1^*, c_2^*) = 0$ (at least in the noiseless case). By this minimization, we have that $\sigma \in SBV(\Omega)$ (σ will be a piecewise-constant function, with the discontinuity set of finite length).

We now introduce an artificial time parameter t and let $\phi(\cdot) = \phi(\cdot, t)$, $c_1 = c_1(t)$ and $c_2 = c_2(t)$. Differentiating the energy, we obtain:

$$\frac{dE}{dt} = \frac{\partial E}{\partial c_1}\frac{dc_1}{dt} + \frac{\partial E}{\partial c_2}\frac{dc_2}{dt} + \int_\Omega \frac{\partial E}{\partial \phi}\frac{d\phi}{dt}\, dx.$$

Furthermore,

$$\begin{aligned} \frac{\partial E}{\partial \phi} &= (1 + \alpha'(F)L)\frac{\partial F}{\partial \phi} + \alpha(F)\frac{\partial L}{\partial \phi} \\ &= (1 + \alpha'(F)L)\frac{\partial F}{\partial \sigma}\frac{\partial \sigma}{\partial \phi} - \alpha(F)\delta(\phi)\nabla\cdot\frac{\nabla\phi}{|\nabla\phi|} \\ &= \delta(\phi)\Big((1 + \alpha'(F)L)(c_2 - c_1)\frac{\partial F}{\partial \sigma} - \alpha(F)\nabla\cdot\frac{\nabla\phi}{|\nabla\phi|}\Big), \end{aligned}$$

and

$$\begin{aligned}\frac{\partial E}{\partial c_1} &= (1+\alpha'(F)L)\int_\Omega \frac{\partial F}{\partial \sigma}\frac{\partial \sigma}{\partial c_1}dx \\ &= (1+\alpha'(F)L)\int_\Omega \frac{\partial F}{\partial \sigma}(1-H(\phi))dx.\end{aligned}$$

Similarly,

$$\frac{\partial E}{\partial c_2} = (1+\alpha'(F)L)\int_\Omega \frac{\partial F}{\partial \sigma}H(\phi)dx.$$

Let u_n and τ_n the n^{th} potential and adjoint potential, so that they respectively solve (1) and (2) with $I = I_n$ and $V = V_n$. It can be shown that the Fréchet derivative of the fitting term is given by (see for example [4] or [12]),

$$\frac{\partial F}{\partial \sigma} = -2\sum_{n=1}^{N}\frac{\nabla u_n \cdot \nabla \tau_n}{N\|V_n\|_2^2}.$$

Thus if we set,

$$\begin{aligned}\frac{d\phi}{dt} &= -\delta(\phi)\Big((1+\alpha'(F)L)(c_2-c_1)\frac{\partial F}{\partial \sigma} - \alpha(F)\nabla\cdot\frac{\nabla\phi}{|\nabla\phi|}\Big), \\ \frac{dc_1}{dt} &= -(1+\alpha'(F)L)\int_\Omega \frac{\partial F}{\partial \sigma}(1-H(\phi))\ dx, \\ \frac{dc_2}{dt} &= -(1+\alpha'(F)L)\int_\Omega \frac{\partial F}{\partial \sigma}H(\phi)\ dx,\end{aligned}$$

we have that $\frac{dE}{dt} \leq 0$. Hence, these equations give the minimization formulation of the inverse conductivity problem.

3 Numerical details and reconstruction results

In the following numerical experiments, we take the domain to be the unit square, $\Omega = [0,1]^2$. To derive the linear system of equations that represents $\nabla \cdot \sigma \nabla$ at the grid points away from the boundary, we look at the integral of equation (1) (or (2)) over a square, P, centered at a grid point (see Figure 1):

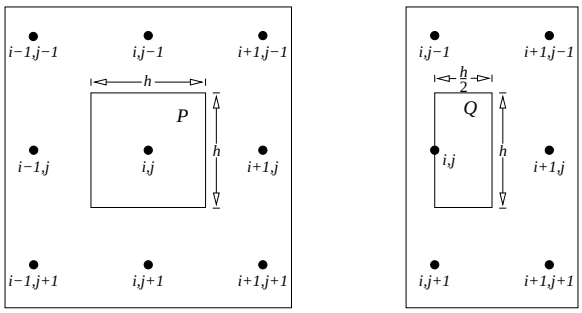

Figure 1: Integration domains.

$$0 = \int_P \nabla \cdot \sigma \nabla u dx = \int_{\partial P} \sigma \frac{\partial u}{\partial n} dS.$$

Using finite differences to approximate the normal derivative of u in this formula, we obtain:

$$\begin{aligned}
0 &= \sigma_{i+\frac{1}{2},j}\big(\frac{u_{i+1,j}-u_{i,j}}{h}\big)h + \ \sigma_{i,j-\frac{1}{2}}\big(\frac{u_{i,j-1}-u_{i,j}}{h}\big)h \\
&\quad + \sigma_{i-\frac{1}{2},j}\big(\frac{u_{i-1,j}-u_{i,j}}{h}\big)h + \ \sigma_{i,j+\frac{1}{2}}\big(\frac{u_{i,j+1}-u_{i,j}}{h}\big)h, \\
0 &= \frac{-(\sigma_{i+\frac{1}{2},j}+\sigma_{i,j-\frac{1}{2}}+\sigma_{i-\frac{1}{2},j}+\sigma_{i,j+\frac{1}{2}})}{h^2}u_{i,j} \\
&\quad + \frac{\sigma_{i+\frac{1}{2},j}}{h^2}u_{i+1,j} + \frac{\sigma_{i,j-\frac{1}{2}}}{h^2}u_{i,j-1} + \frac{\sigma_{i-\frac{1}{2},j}}{h^2}u_{i-1,j} + \frac{\sigma_{i,j+\frac{1}{2}}}{h^2}u_{i,j+1}.
\end{aligned}$$

At the boundary nodes, but not the corner nodes, we use the boundary condition,

$$\sigma \frac{\partial u}{\partial n} = f,$$

where f is either I or $u|_{\partial\Omega} - V$, and we integrate over a domain, Q, (see Figure 1):

$$\begin{aligned}
0 &= \int_Q \nabla \cdot \sigma \nabla u dx = \int_{\partial Q} \sigma \frac{\partial u}{\partial n} dS \\
&= \sigma_{i+\frac{1}{2},j}\big(\frac{u_{i+1,j}-u_{i,j}}{h}\big)h + \ \sigma_{i,j-\frac{1}{2}}\big(\frac{u_{i,j-1}-u_{i,j}}{h}\big)\frac{h}{2} \\
&\quad + f_{i,j}h + \ \sigma_{i,j+\frac{1}{2}}\big(\frac{u_{i,j+1}-u_{i,j}}{h}\big)\frac{h}{2}, \\
-\frac{f_{i,j}}{h} &= \frac{-(2\sigma_{i+\frac{1}{2},j}+\sigma_{i,j-\frac{1}{2}}+\sigma_{i,j+\frac{1}{2}})}{2h^2}u_{i,j} \\
&\quad + \frac{2\sigma_{i+\frac{1}{2},j}}{2h^2}u_{i+1,j} + \frac{\sigma_{i,j-\frac{1}{2}}}{2h^2}u_{i,j-1} + \frac{\sigma_{i,j+\frac{1}{2}}}{2h^2}u_{i,j+1}.
\end{aligned}$$

In a similar fashion, we obtain the equations at the four corner nodes. Note that in this discretization of the operator, we need the values of the conductivity at points which lie in between the grid points. We take its value to be the minimum of the two nearest values to preserve the discontinuous nature of σ. This approximation ignores isolated points, where σ is bigger than at its surrounding neighbors. This is taken into consideration in evaluating dc/dt and in re-normalizing ϕ.

We will assume that the conductivity constant $c_1^* = 1$ is fixed and that it is the value of σ^* on the boundary of the domain. In this case, the evolution equations for ϕ and the unknown conductivity constant $c_2 = c$ are given by:

$$\frac{d\phi}{dt} = -\delta(\phi)\Big((1+\alpha'(F))(c-1)\frac{\partial F}{\partial \sigma} - \alpha(F)\nabla \cdot \frac{\nabla \phi}{|\nabla \phi|}\Big), \tag{7}$$

$$\frac{dc}{dt} = -(1+\alpha'(F)L)\int_\Omega \frac{\partial F}{\partial \sigma} H(\phi)\ dx. \tag{8}$$

Following [10], we use a semi-implicit finite-difference scheme to discretize the $\nabla \cdot \frac{\nabla \phi}{|\nabla \phi|}$ term. Since we are assuming that one of the values of the conductivity is known, we impose Dirichlet boundary conditions on ϕ. We use the approximations of the Heaviside and Dirac delta functions given in [9], [10],

$$H_\epsilon(x) = \frac{1}{2}\Big[1 + \frac{2}{\pi}\arctan\Big(\frac{x}{\epsilon}\Big)\Big], \quad \delta_\epsilon(x) = \frac{1}{\pi}\frac{\epsilon}{\epsilon^2 + x^2}.$$

To compute the Fréchet derivative of the fitting term, we need the potential and the adjoint potential in Ω for each one of the configurations. To find these potentials, we use the conjugate gradient method to solve the system of linear equations that results from the finite volume discretization of (1) and (2). In discretizing the $\nabla \cdot \sigma \nabla$ operator, we also use the above approximations, H_ϵ and δ_ϵ. However, since the finite volume discretization requires the values of σ at the half grid points, we take its value to be the minimum of the two nearest values to preserve the discontinuous nature of σ, as explained before.

Since there is no analytic solution to the equation that governs the evolution of c, the differential equation (8) has to be solved numerically. However, instead of integrating this equation, we evaluate $\frac{dc}{dt}$ nearby the previous value of c and approximate $\frac{dc}{dt}$ by a quadratic polynomial. The next value of c is taken to be the value that minimizes the absolute value of this polynomial (if there are two such points, we take the one closest to the previous value). We alternate minimizing the functional with respect to ϕ and c.

To generate artificial data, we compute the Neumann-to-Dirichlet map, Λ_{σ^*}, by applying the conjugate gradient method to the finite volume discretization of the forward problem. The Neumann boundary data are chosen to be sines and cosines of higher and higher frequency on the boundary.

For the cases with regularizations, we use

$$\alpha(F) = \frac{10^{-7}}{\pi} \arctan(10^7 F),$$

and for no regularization, we use $\alpha(F) = 0$.

3.1 Test 1 – Two Inclusions

The true conductivity for this experiment has two inclusions (see Figure 2). Both inclusions have conductivity $c_2^* = 2$ and the background conductivity $c_1^* = 1$. The reconstructions in Figure 4 were carried out using 6 configurations both with regularization and without regularization. Figure 5 shows the same reconstructions using 12 configurations. We also show the value of the fidelity term $F(t)$ versus iteration number. The overall behavior of the total energy $E(t)$ is qualitatively very similar to the behavior of the fidelity term. The final values from the minimization are listed in Table 1.

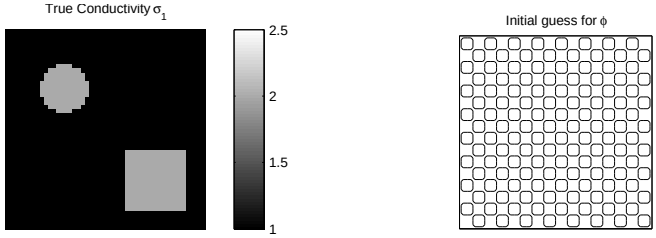

Figure 2: The true conductivity σ_1^* and the initial guess for ϕ. The conductivity has two inclusions, a square and a circle. The initial guess for the unknown conductivity constant c is 1.

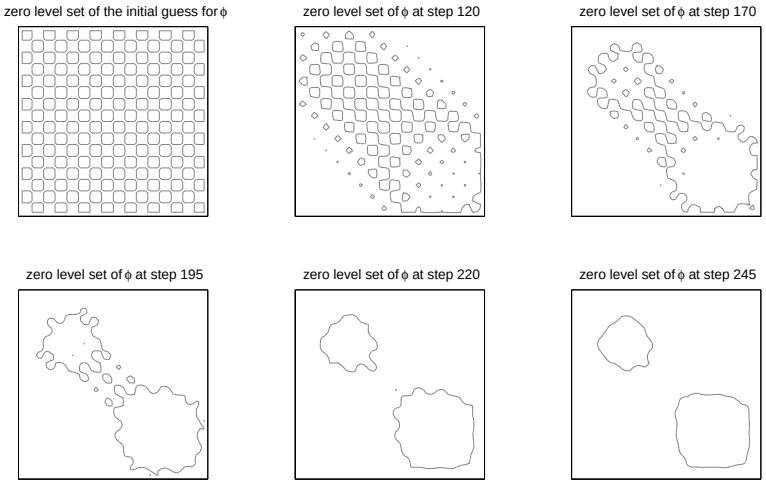

Figure 3: Evolution of the zero level line of ϕ over time for the $N = 6$ case with regularization.

	N	c	F
without regularization	6	2.0219	$2.6691 * 10^{-8}$
with regularization	6	2.0256	$2.8221 * 10^{-8}$
without regularization	12	2.1400	$3.8258 * 10^{-8}$
with regularization	12	2.0270	$5.1410 * 10^{-8}$

Table 1: Final values for the various test 1 reconstructions.

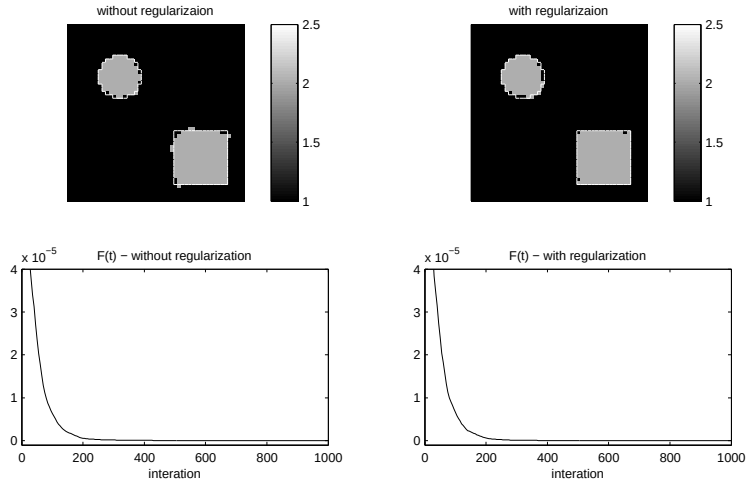

Figure 4: Reconstructions of σ_1^* for $N = 6$, without regularization (left) and with regularization (right). The white line outlines the true location of the inclusions. The final values are listed in Table 1.

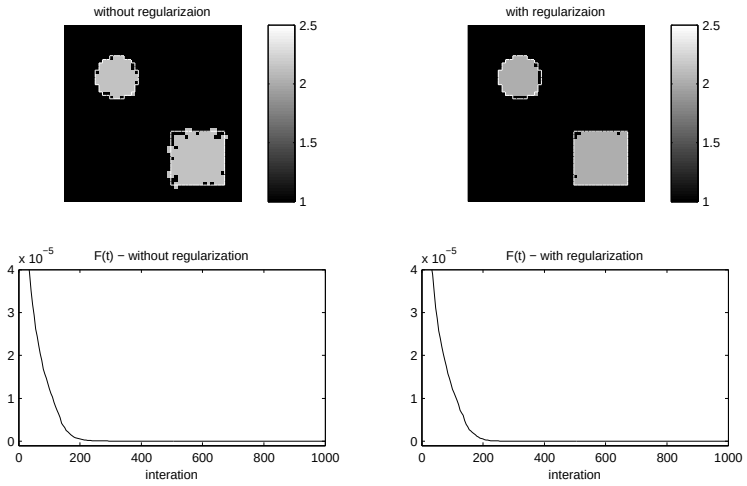

Figure 5: Reconstructions of σ_1^* for $N = 12$, without regularization (left) and with regularization (right). The white line outlines the true location of the inclusions. The final values are listed in Table 1.

3.2 Test 2 – Inclusion with an Empty Interior

The true conductivity for this experiment has an inclusion that contains a hole (see Figure 6). The inclusion has a conductivity $c_2^* = 2$ and the background conductivity $c_1^* = 1$. The reconstructions in Figure 7 were carried out using 6 configurations both with regularization and without regularization. Figure 8 shows the same reconstructions using 12 configurations. The final values from the minimization are listed in Table 2.

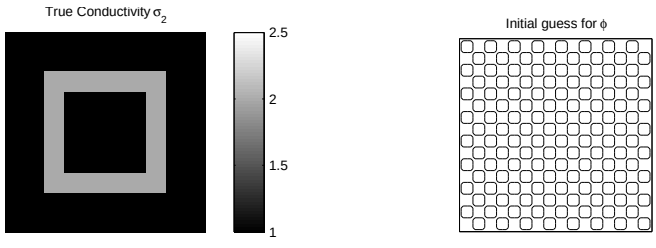

Figure 6: The true conductivity σ_2^* and the initial guess for ϕ. The conductivity has an inclusion with an empty interior. The initial guess for the unknown conductivity constant c is 1.

	N	c	F
without regularization	6	2.1517	$6.7434 * 10^{-8}$
with regularization	6	1.8598	$3.7849 * 10^{-8}$
without regularization	12	2.3290	$5.1093 * 10^{-8}$
with regularization	12	2.0335	$4.0141 * 10^{-8}$

Table 2: Final values for the various test 2 reconstructions.

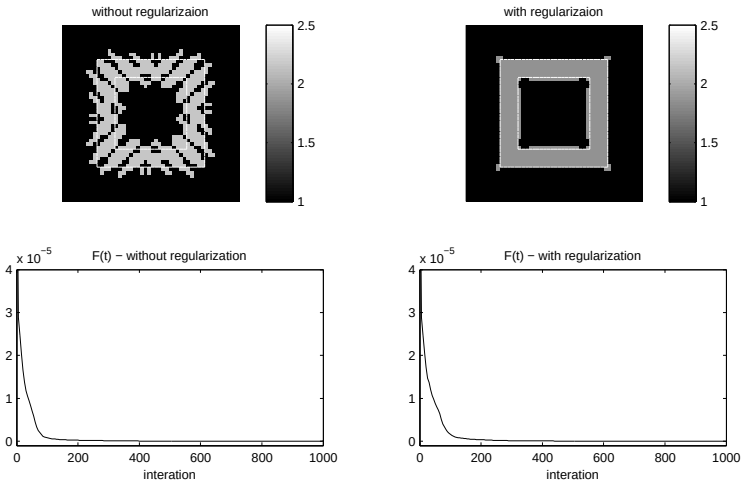

Figure 7: Reconstructions of σ_2^* for $N = 6$, without regularization (left) and with regularization (right). The white line outlines the true location of the inclusion. The final values are listed in Table 2.

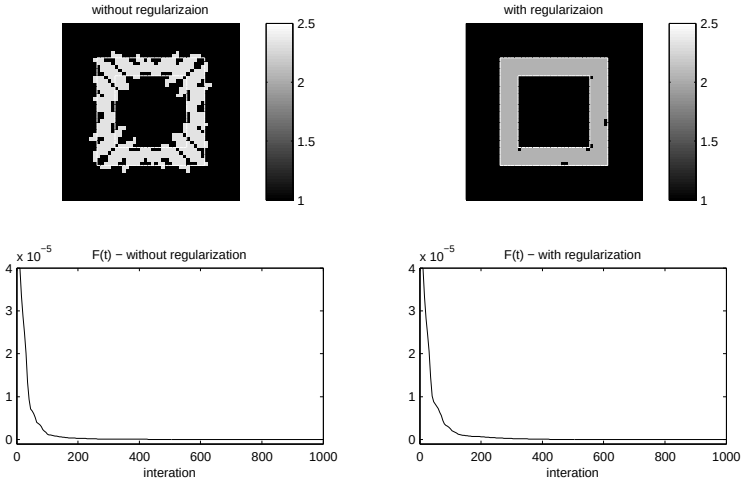

Figure 8: Reconstructions of σ_2^* for $N = 12$, without regularization (left) and with regularization (right). The white line outlines the true location of the inclusion. The final values are listed in Table 2.

3.3 Test 3 – Noise

For this experiment, we use the true conductivity σ_1^* of test 1. However, the measurements V_n are corrupted with additive uniformly distributed noise, that is,

$$V_n^c = (1 + \epsilon s_n)V_n,$$

where s_n is a function on the boundary of Ω that takes on random values between $[-1, 1]$ and ϵ controls the size of noise. Figure 9 shows regularized reconstructions of σ_1^* with $N = 12$ and noisy data with $\epsilon = .01$ and $\epsilon = .05$, while the final values are given in Table 3.

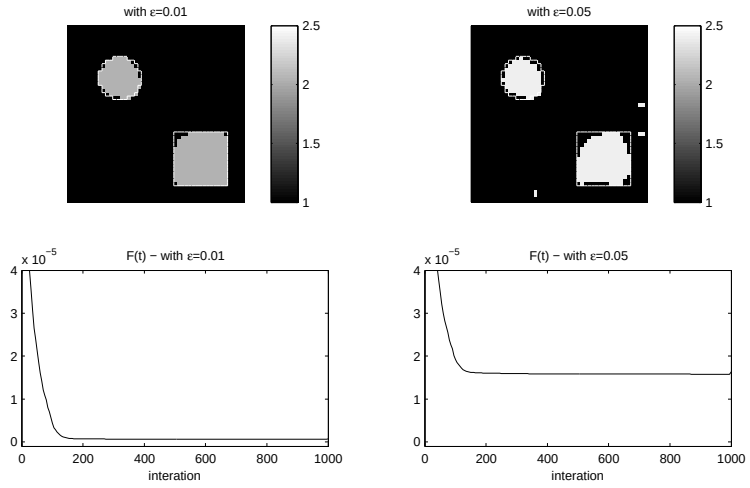

Figure 9: Reconstructions of σ_1^* for $N = 12$ with regularization for noisy data with $\epsilon = .01$ (left) and $\epsilon = .05$ (right).

	N	c	F
$\epsilon = 0.01$	12	2.0363	$7.2851 * 10^{-7}$
$\epsilon = 0.05$	12	2.3865	$1.6377 * 10^{-5}$

Table 3: Final values for the various test 3 reconstructions.

References

[1] L. Ambrosio and V.M. Tortorelli, *On the approximation of free discontinuity problems*, Bollettino della Unione Matematica Italiana, **6B** (1992), 105–123.

[2] K. Astala and L. Paivarinta, *Calderón's inverse conductivity problem in the plane*, Annals of Mathematics, **163** (2006), 265–299.

[3] L. Borcea, *Electrical impedance tomography*, Inverse Problems, **18** (2002), R99–R136.

[4] L. Borcea, G.A. Gray and Y. Zhang, *Variationally constrained numerical solution of electrical impedance tomography*, Inverse Problems, **19** (2003), 1159–1184.

[5] L. Borcea, J.G. Berryman, G.C. Papanicolaou, *High-contrast impedance tomography*, **12** (1996), 835–858.

[6] R.M. Brown and G.A. Uhlmann, *Uniqueness in the inverse conductivity problem for nonsmooth conductivities in two dimensions*, Communications in Partial Differential Equations, **2** (1997), 1009–1027.

[7] M. Burger, *A level set method for inverse problems*, Inverse Problems, **17** (2001), 1327–1355.

[8] A.-P. Calderón, *On an inverse boundary value problem*, Seminar on Numerical Analysis and its Applications to Continuum Physics (Rio de Janeiro, 1980), Soc. Brasil. Mat. (1980), 65–73.

[9] T.F. Chan and L. Vese, *An active contour model without edges*, LNCS, **1682** (1999), 141–151.

[10] T.F. Chan and L.A. Vese, *Active Contours Without Edges*, IEEE Transactions on Image Processing, **10** (2001), 266–277.

[11] T.F. Chan and X.-C. Tai, *Level Set and Total Variation Regularization for Elliptic Inverse Problems With Discontinuous Coefficients,*, UCLA CAM Report, 03-15, 2003.

[12] E.T. Chung, T.F. Chan and X.C. Tai, *Electrical impedance tomography using level set representation and total variational regularization*, Journal of Computational Physics, **205** (2005), 357–372.

[13] A. Dervieux and F. Thomasset, *A finite element method for the simulation of Rayleigh-Taylor instability*, Lecture Notes in Mathematics, **771** (1979), 145–159.

[14] A. Dervieux and F. Thomasset, *Multifluid incompressible flows by a finite element method*, Lecture Notes in Physics, **141** (1980), 158–163.

[15] R. Kohn and M. Vogelius, *Determining conductivity by boundary measurements*, Communications on Pure and Applied Mathematics, **37** (1984), 289–298.

[16] R. Kohn and M. Vogelius, *Determining conductivity by boundary measurements 2. Interior results*, Communications on Pure and Applied Mathematics, **38** (1985), 643–667.

[17] B. Kortschak, H. Wegleiter and B. Brandstatter, *Formulation of cost functionals for different measurement principles in nonlinear capacitance tomography*, Measurement Science & Technology, **18** (2007), 71–78.

[18] B. Kortschak and B. Brandstatter, *A FEM-BEM approach using level-sets in electrical capacitance tomography*, COMPEL-The International Journal for Computation and Mathematics in Electrical and Electronic Engineering, **24** (2005), Sp. Iss. SI, 591–605.

[19] D. Mumford and J. Shah, *Optimal approximations by piecewise smooth functions and associated variational problems*, Communications on Pure and Applied Mathematics, **42** (1989), 577–685.

[20] A.I. Nachman, *Global uniqueness for a two-dimensional inverse boundary value problem*, Annals of Mathematics, **143** (1996), 71–96.

[21] L.K. Nielsen, X.C. Tai, S.I. Aanonsen SI and M. Espedal, *A binary level set model for elliptic inverse problems with discontinuous coefficients*, International Journal of Numerical Analysis and Modeling, **4** (2007), 74–99.

[22] S. Osher and J.A. Sethian, *Fronts propagating with curvature-dependent speed - Algorithms based on Hamilton-Jacobi formulations*, Journal of Computational Physics, **79** (1988), 12–49.

[23] L. Paivarinta, A. Panchenko and G. Uhlmann, *Complex geometrical optics solutions for Lipschitz conductivities*, Revista Matematica Iberoamericana, **19** (2003), 57–72.

[24] L. Rondi and F. Santosa, *Enhanced electrical impedance tomography via the Mumford-Shah functional*, ESAIM-Control Optimisation and Calculus of Variations, **6** (2001), 517–538.

[25] C. Samson, L. Blanc-Féraud, G. Aubert and J. Zerubia, *A level set model for image classification*, International Journal of Computer Vision, **40** (2000), 187–197.

[26] M. Soleimani, O. Dorn and W.R.B. Lionheart, *A narrow-band level set method applied to EIT in brain for cryosurgery monitoring*, IEEE Transactions on Biomedical Engineering, **53** (2006), 2257–2264.

[27] J. Sylvester and G. Uhlmann, *A global uniqueness theorem for an inverse boundary-value problem*, Annals of Mathematics, **125** (1987), 153–169.

[28] P. Neittaanmaki, J. Sprekels, and D. Tiba, "Optimization of Elliptic Systems: Theory and Applications," Springer Monographs in Mathematics, 2005.

[29] A. Tsai, A. Yezzi, and A.S. Willsky, *Curve evolution implementation of the Mumford-Shah functional for image segmentation, denoising, interpolation, and magnification*, IEEE Transactions on Image Processing, **10** (2001), 1169–1186.

[30] L.A. Vese and T.F. Chan, *A Multiphase Level Set Framework for Image Segmentation Using the Mumford and Shah Model*, International Journal of Computer Vision, **50** (2002), 271–293.

[31] H.K. Zhao, T. Chan, B. Merriman, and S. Osher, *Variational level set approach to multiphase motion*, Journal of Computational Physics, **127** (1996), 179–195.

E-mail address: nicktan@math.ucla.edu
E-mail address: lvese@math.ucla.edu